Machine learning-driven QSAR models for predicting the mixture toxicity of nanoparticles

Zhang, F.; Wang, Z.; Peijnenburg, W.J.G.M.; Vijver, M.G.

Environment International 177 (2023) 108025

Contents lists available at ScienceDirect

Environment International

journal homepage: www.elsevier.com/locate/envint

Full length article

Machine learning-driven QSAR models for predicting the mixture toxicity of nanoparticles

Fan Zhang [a], Zhuang Wang [b], Willie J.G.M. Peijnenburg [a,c,*], Martina G. Vijver [a]

[a] Institute of Environmental Sciences (CML), Leiden University, Leiden 2300 RA, the Netherlands
[b] School of Environmental Science and Engineering, Collaborative Innovation Center of Atmospheric Environment and Equipment Technology, Jiangsu Key Laboratory of Atmospheric Environment Monitoring and Pollution Control, Nanjing University of Information Science and Technology, Nanjing 210044, PR China
[c] Centre for Safety of Substances and Products, National Institute of Public Health and the Environment (RIVM), Bilthoven 3720 BA, the Netherlands

ARTICLE INFO

Handling Editor: Adrian Covaci

Keywords:
Nanotoxicity
Advanced nanomaterials
Support vector machine
Neural network
Mixture toxicity

ABSTRACT

Research on theoretical prediction methods for the mixture toxicity of engineered nanoparticles (ENPs) faces significant challenges. The application of *in silico* methods based on machine learning is emerging as an effective strategy to address the toxicity prediction of chemical mixtures. Herein, we combined toxicity data generated in our lab with experimental data reported in the literature to predict the combined toxicity of seven metallic ENPs for *Escherichia coli* at different mixing ratios (22 binary combinations). We thereafter applied two machine learning (ML) techniques, support vector machine (SVM) and neural network (NN), and compared the differences in the ability to predict the combined toxicity by means of the ML-based methods and two component-based mixture models: independent action and concentration addition. Among 72 developed quantitative structure–activity relationship (QSAR) models by the ML methods, two SVM-QSAR models and two NN-QSAR models showed good performance. Moreover, an NN-based QSAR model combined with two molecular descriptors, namely enthalpy of formation of a gaseous cation and metal oxide standard molar enthalpy of formation, showed the best predictive power for the internal dataset ($R^2_{test} = 0.911$, adjusted $R^2_{test} = 0.733$, $RMSE_{test} = 0.091$, and $MAE_{test} = 0.067$) and for the combination of internal and external datasets ($R^2_{test} = 0.908$, adjusted $R^2_{test} = 0.871$, $RMSE_{test} = 0.255$, and $MAE_{test} = 0.181$). In addition, the developed QSAR models performed better than the component-based models. The estimation of the applicability domain of the selected QSAR models showed that all the binary mixtures in training and test sets were in the applicability domain. This study approach could provide a methodological and theoretical basis for the ecological risk assessment of mixtures of ENPs.

1. Introduction

The unique physicochemical features of nanostructured materials make them particularly appealing for specific applications (Wyrzykowska et al., 2022). Developments go with a fast pace, with first-generation nanomaterials (NMs) already embedded in a variety of products and advanced NMs such as nanocomposites continuously generated (Jayaramulu et al., 2022). With the continuous development and application of NMs, different types of engineered nanoparticles (ENPs) will now be co-discharged into the environment. Municipal wastewater treatment facilities and sewage systems are becoming crucial intermediary routes for the release of the mixtures of ENPs into the environment (Georgantzopoulou et al., 2020; Simelane and Dlamini, 2019; Singh and Kumar, 2020). It is expected that industrial and municipal wastewater are a major source of mixtures of ENPs of different compositions. As a consequence, a wide range of structurally and chemically diverse ENPs will unavoidably be released into the environmental compartments (Hong et al., 2021), raising worries about potential ENPs-induced human and ecological impacts (Avellan et al., 2021). This requires to explore the scientific challenge of assessing mixture toxicity of multiple ENPs (Zhang et al., 2022a).

Fortunately experimental data on the mixture toxicity of ENPs is expanding quite recently, while progress on methods for evaluating and predicting the mixture toxicity of ENPs is lagging (Zhang et al., 2022a). Enabling ENPs' mixture predictions, classical component-based mixture models have been used (Lopes et al., 2016; Martín-de-Lucía et al., 2019).

* Corresponding author at: Institute of Environmental Sciences (CML), Leiden University, Leiden 2300 RA, the Netherlands.
E-mail address: peijnenburg@cml.leidenuniv.nl (W.J.G.M. Peijnenburg).

https://doi.org/10.1016/j.envint.2023.108025
Received 5 February 2023; Received in revised form 7 May 2023; Accepted 6 June 2023
Available online 9 June 2023

However, these mixture models such as concentration addition (CA), independent action (IA), and a combination of the two models rely on the assessment of the concentration–response relationship of the single components and on the identification of the toxic mode of action of the single components (Zhang et al., 2021). *In silico* predictive toxicology appears to be a promising alternative to the mixture modeling. Among the novel approach methodologies based on *in silico* predictions, quantitative structure–activity relationships (QSAR) modeling proves to be a useful tool for the prediction of the biological activity or property of a compound by providing a mathematical correlation with its structural features (Tropsha, 2010). Recently, QSAR methods are being applied in methodological studies for the quantitative prediction of the toxicity of mixtures of ENPs (Kar et al., 2022; Mikolajczyk et al., 2016; Na et al., 2023; Zhang et al., 2022b). Meanwhile, machine learning (ML) methods, which seek to construct an explicit or implicit model based on current data (known as training data) to make predictions or decisions on complicated issues (Wang et al., 2021), have already stepped into the spotlight for *in silico* prediction of toxicology. ML methods to date have shown unprecedented predictive power in predicting the toxicity of ENPs (Balraadjsing et al., 2022; Ji et al., 2022; Jia et al., 2021; Trinh et al., 2022). Thus, ML-powered QSAR modeling approaches could be a strong tool to deal with the problem of predicting the toxicity of mixtures of ENPs, and would perform better and more cost-effective than the classical mixture models. However, there is still a scarcity of QSAR models based on ML approaches for predicting the mixture toxicity of multiple ENPs.

The present study aimed at rebuilding existing QSAR for use with NMs (nano-QSAR) by incorporating ML methods to describe the toxicity of a mixture of ENPs and comparing the performance with the mixture models. This enables the understanding of the link between the physicochemical properties describing the components in the mixture and the cytotoxicity of 22 binary mixtures of metal oxide nanoparticles (MO_X NPs) against *Escherichia coli*, a commonly used bacterium species in toxicity screening. Toxicity data for 12 binary mixtures with two different mixing ratios from our laboratory were used as an internal dataset. Toxicity data for 10 binary mixtures with another mixing ratio from the literature were used as an external dataset. The selected ML methods, namely support vector machine (SVM) (Ban et al., 2022; Liu et al., 2013) and neural network (NN) (Yang et al., 2022), are well-known and commonly utilized ML algorithms. The study involves eight indicative physicochemical parameters implicated in the mechanism of toxicity of MO_X NPs: surface charge, dispersion stability, dissolution, oxidative stress, and particle reactivity. Then, for the first time, SVM- and NN-based QSAR models for predicting the cytotoxicity of mixtures of individual MO_X NPs with diverse metal elements and different mixture ratios were developed. The goal of this study is to develop a rapid and cost-effective model for predicting the toxicity of mixtures of ENPs and provide a more suitable method for the risk assessment of multiple ENPs.

2. Materials and methods

2.1. Experimental sections

2.1.1. Test materials

CuO NPs with a primary size of 40 nm (advertised specific surface area > 10 m^2/g; purity 99 %), ZnO NPs with a primary size of 14 nm (advertised specific surface area of 30 ± 5 m^2/g; purity > 99 %), TiO_2 NPs with a primary size of 21 ± 5 nm (advertised specific surface area 50 ± 10 m^2/g; purity > 99.5 %), and ZrO_2 NPs with a primary size of 5–25 nm (advertised specific surface area 130 ± 20 m^2/g; purity > 97.2 %) were purchased from PlasmaChem GmbH (Berlin, Germany). The MO_X stock suspensions were freshly prepared in pure water after 30 min sonication in a water bath sonicator and then stored at 4 °C until use.

2.1.2. Physicochemical analysis

Zeta potential (ζP) and hydrodynamic diameters (D_H) of the MO_X NP suspensions at 10 mg/L were analyzed in water using a ZetaSizer instrument (Nano ZS90, Malvern Instruments Ltd., Worcestershire, UK).

2.1.3. Toxicity testing

Cytotoxicity tests were performed with *E. coli* using the microtitration plate assay (Patton et al., 2006). The initial number of bacteria was set at 1×10^8 cells/mL. Bacterial solution after exposure to the test materials was added into a 96-well white flat-bottom microplate, which subsequently was maintained at 37 °C with shaking incubation for 12 h in a constant temperature shaker. Bacteria were exposed to increasing concentrations of the suspensions of CuO NPs (from 1.26×10^{-4} to 3.02×10^{-3} mol/L), ZnO NPs (from 6.14×10^{-5} to 6.76×10^{-4} mol/L), TiO_2 NPs (from 3.76×10^{-4} to 3.76×10^{-3} mol/L), and ZrO_2 NPs (from 4.06×10^{-4} to 9.74×10^{-3} mol/L). Each test concentration was replicated four times. The optical density (OD) values corresponding to the cell number of *E. coli* were monitored using an enzyme-labeled instrument (Thermo Multiskan FC, USA), and the inhibition rate was calculated from the measured OD values. The cytotoxicity of the tested materials was expressed in terms of effect concentrations (EC_{50} and EC_{10}: the effective concentration of a toxicant that induces 50 and 10 % bacteria inhibition), which were calculated using a concentration–response curve (CRC). For the binary mixtures in the internal dataset, *E. coli* cells were treated with various concentrations of MO_X NPs with a fixed mixture ratio, where the first and second mixtures were based on the initial EC_{50} and the EC_{10} of each MO_X NP, respectively. Thus, the two mixtures were named Int ($R1$) mixture and Int ($R2$) mixture.

2.2. Computational methods

2.2.1. Determination of concentration–response curve

The Logistic regression model, as shown in Eq. (1), was used to fit the CRCs for single and binary MO_X NPs.

$$E = \frac{100}{\left(1 + \left(\frac{C}{EC_{50}}\right)^{\theta}\right)} \tag{1}$$

where E is the effect confined to the range of 0–100 %, C is the exposure concentration of the test materials, and θ represents the slope parameter.

2.2.2. Joint effect modeling

As the most representative approaches used are the IA and CA models (Bliss, 1939; Loewe and Muischneck, 1926), which were applied to predict the toxicity (denoted EC_{50} values) of the mixtures of MO_X NPs. Throughout the modeling EC_{50} values were transformed to inverted logarithm i.e., $\log 1/EC_{50}$.

The general equation shown in Eq. (2) was used for the IA model,

$$E(C_{\text{mix}}) = 1 - \prod_{i=1}^{n}(1 - E(C_i)) \tag{2}$$

where $E(C_{\text{mix}})$ is the effect expected at the total concentration of the mixture (scaled between 0 and 100 %) and $E(C_i)$ is the effect that the ith mixture component would provoke if applied singly at concentration C_i.

The total concentration of a mixture causing x % effect ($EC_{x\text{mix}}$) was calculated from the CRC of the individual component using the CA model, as shown in Eq. (3),

$$EC_{xmix} = \left(\sum_{i=1}^{n}\frac{P_i}{EC_{xi}}\right)^{-1} \tag{3}$$

where P_i is the fraction of component i in the mixture and EC_{xi} is the concentration of component i that would result in x % effect if used alone.

2.2.3. Construction of datasets

Two datasets were constructed for the development and validation of the predictive models. The dataset was chosen not only to take into account data sample diversity (i.e., diversity of mixed components and mixed concentration ratios), but also to reduce the variability of inter-laboratory toxicity testing conditions. The first dataset (named internal dataset) consists of experimental data from our laboratory. The internal dataset consists of 12 data rows, consisting of the binary mixtures of four MO_X NPs (CuO, ZnO, TiO_2, and ZrO_2) at two different mixture ratios. The results of physicochemical analysis which included the assessment of the ζP and the D_H of MO_X NPs in the single and binary mixture systems and the CRCs for the mixtures obtained from the *E. coli* toxicity testing and predicted by the IA and CA models are described in the Supplementary material.

The second dataset (named combined dataset) comprised both internal data and external data. The external data of the toxicity of 10 binary mixtures of five MO_X NPs (Al_2O_3, Fe_2O_3, SiO_2, TiO_2, and ZnO) to *E. coli* was collected from Kar et al. (2022). The binary nano-mixtures in the external dataset and the internal dataset have both different kinds of combinations and different mixture ratios of components between them. The external dataset was named Ext (*R*3) mixture. The combined dataset has a total of 22 data rows.

2.2.4. Calculation of mixture descriptors

A mixture descriptor (D_{mix}) is a weighted descriptor that quantifies how much each component contributes to the overall activity of a mixture (Altenburger et al., 2003). D_{mix} has been practically applied in the toxicity prediction studies of ENP mixtures (Kar et al., 2022; Trinh et al., 2022). D_{mix} is expressed by arithmetic mean (Eq. (4)):

$$D_{mix} = x_i D_i + x_j D_j \quad (4)$$

where x_i and x_j are the mole fractions of constituent *i* and *j* in the mixtures, and D_i and D_j are descriptors of the individual MO_X NPs. The selected descriptors of the individual MO_X NPs and the calculated D_{mix} based on Eq. (4) are shown in Table S1 and in Table S2, respectively. In the selection of descriptors for the individual MO_X NPs, we referred to the qualities summarized by Roy et al. (2015). Moreover, the selected descriptors are universal descriptors, which are effectively used to construct QSAR models of individual MO_X NPs. Furthermore, these descriptors not only reflect the characteristics of nanostructures but also directly respond to toxicologically relevant properties. In details, there were eight descriptors of the individual MO_X NPs from three different types: two periodic table-based descriptors (electronegativity of metal atoms, χ_{me} and sum of metal electronegativity for an individual metal oxide divided by the number of oxygen atoms present in a particular metal oxide, $\Sigma\chi_{me/nO}$) derived from the publicly available periodic table information (Kar et al., 2014), two experimental descriptors (ζP and D_H) determined in our laboratory (CuO, ZnO, TiO_2, and ZrO_2 NPs) and obtained from a previous study (Al_2O_3, Fe_2O_3, SiO_2, TiO_2, and ZnO NPs) (Kar et al., 2022), three metal oxide energy descriptors including the enthalpy of formation of a gaseous cation having the same oxidation state as the oxidation state of the metal in the metal oxide structure (ΔH_{me+}) (Puzyn et al., 2011), the metal oxide standard molar enthalpy of formation (ΔH_{sf}) (Haynes, 2011), and the energy of the conduction band (E_C) (Zhang et al., 2012) of the nanoparticle, as well as the ionic index of the metal cation (Z^2/r) (Walker et al., 2003). Stepwise multiple linear regression in SPSS 23.0 was used to perform a preliminary screening of the descriptions obtained, and the *t* value was selected to determine the comparative importance of the descriptors on the toxic effect concentrations ($\log 1/EC_{50}$) of binary mixtures of MO_X NPs.

2.2.5. Machine learning-based modeling

Two popular ML algorithms, namely SVM and NN, were used to develop the QSAR models for predicting the toxicity of binary mixtures of MO_X NPs. The datasets were divided into training (60 % data) and test (40 % data) sets at random. For the SVM algorithm, the Gaussian radial basis function (RBF) was used. For the NN algorithm, the hyperbolic tan function for the hidden layer and the quasi-Newton method for weight optimization were applied. We used the data mining toolbox in Python for developing the ML-based predictive models (Demšar et al., 2013). To validate the models, the squared correlation coefficient (R^2) and the adjusted squared correlation coefficient (R^2_{adj}) between observed and predicted $\log 1/EC_{50}$, the root mean square error (RMSE), and the mean absolute error (MAE) of the training and test datasets were used. These statistical parameters are commonly used in current nano-QSAR studies and are widely accepted (Gajewicz et al., 2015; Kar et al., 2022; Trinh et al., 2022). Randomization tests proposed for testing the robustness of the selected models were performed using the metric $^cR^2_P$ (Kar et al., 2014). If the $^cR^2_P$ value is more than the stipulated threshold value of 0.5 then an acceptable model has been developed. The second-order bias-corrected Akaike Information Criterion (*AICc*) index as an additional statistical measure was employed on the full set to evaluate the relationship between variables. The *AICc* value was calculated using *R* software.

2.2.6. Applicability domain

The OECD principles of QSAR validation recommend that: *A (Q)SAR should be associated with a defined domain of applicability* (OECD, 2014). The function of the applicability domain (AD) is to define the compounds that can be reliably predicted by the QSAR model, which can also be understood as the set of compounds to which the model applies. The AD in this work was generated by using the Student's *t*-distribution on Euclidean distances (structural domain) and standardized residuals (response domain) of a training dataset to define the space where accurate predictions can be made with a specified level of confidence (Gajewicz, 2018).

3. Results and discussion

3.1. Toxicity of binary ENP mixtures

CRCs established for the binary mixtures of CuO, ZnO, TiO_2, and ZrO_2 NPs are shown in Figure S1. Based on the curves, the $\log 1/EC_{50}$ values were determined and these are summarized in Table 1. For the binary mixtures with a certain mixture ratio, TiO_2 and ZrO_2 NPs induced the least toxicity in the combined exposure setting. Comparative analysis also revealed that the toxicity of CuO NPs combined with ZnO or TiO_2 NPs was higher than for other binary combinations.

3.2. Machine learning-based QSAR prediction

Based on the ML methods, 72 QSAR models integrating different D_{mix} (Fig. 1) were developed. The performance of 36 SVM- and 36 NN-based QSAR models is shown in Tables S3 and S4, respectively. We selected a good prediction model according to the following three criteria: (i) $R^2 \geq 0.81$ for *in vitro* data (Kubinyi, 1993); (ii) adjusted $R^2 > 0.60$ (Olasupo et al., 2020); (iii) the above two conditions need to be satisfied not only for both the training and the test sets but also for both the internal and combined datasets, as well as for both the SVM- and NN-based models when applying the same descriptors. Among the developed QSAR models, two SVM-based models (S12 and S31) and two NN-based models (N12 and N31) performed comparably better than other models for both the internal and combined datasets. This also means that the selected QSAR models can reliably predict the toxicity of mixtures of individual MO_X NPs under multiple different experimental conditions.

Moreover, the predicted $\log 1/EC_{50}$ values by the good models (S12, S31, N12, and N31) are shown in Table 1 (the internal dataset) and in Table 2 (the combined dataset). The percental difference averaged between the experimental and predicted values by the selected models for the internal and combined datasets was 2.34, 2.50, 1.08, 1.04 and 7.16, 7.29, 2.87, 2.61 % respectively. In addition, the obtained $^cR^2_P$ values for

Table 1
Toxicity data of binary mixtures of MO_X NPs for the internal dataset [a].

Mixture system of MO_X NPs	Observed log1/EC_{50} (mol/L)	Predicted log1/EC_{50} (mol/L) QSAR models				Mixture models	
		S12	S31	N12	N31	IA	CA
Int (*R*1)							
CuO + ZnO NPs	2.72	2.68	2.70	2.72	2.72	2.85	3.05
TiO_2 + ZrO_2 NPs	2.10	2.14	2.13	2.10	2.10	2.32	2.44
ZnO + TiO_2 NPs	2.17	2.20	2.18	2.18	2.18	2.96	3.00
ZnO + ZrO_2 NPs*	2.30	2.23	2.14	2.37	2.37	2.39	2.54
CuO + TiO_2 NPs*	2.77	2.81	2.80	2.88	2.80	2.70	2.80
CuO + ZrO_2 NPs	2.29	2.25	2.27	2.29	2.29	2.30	2.46
Int (*R*2)							
CuO + ZnO NPs*	2.82	2.68	2.70	2.69	2.66	2.92	3.15
TiO_2 + ZrO_2 NPs*	2.11	2.14	2.13	2.11	2.10	2.32	2.44
ZnO + TiO_2 NPs	2.20	2.21	2.18	2.19	2.18	2.77	3.05
ZnO + ZrO_2 NPs	2.37	2.23	2.14	2.37	2.37	2.39	2.54
CuO + TiO_2 NPs	2.74	2.71	2.72	2.75	2.75	2.70	2.80
CuO + ZrO_2 NPs	2.14	2.21	2.18	2.14	2.15	2.31	2.41

[a] * indicates the test data.

the selected models via the Y-randomization test are higher than 0.5 (Tables S5 and S6), demonstrating that the models were not created randomly and that they are robust.

Experimentally determined log1/EC_{50} are plotted against predicted log1/EC_{50} for the internal and combined datasets (Fig. 2 and Fig. 3, respectively). The green dotted line indicates that the experimental and the predicted values correspond exactly. The blue straight line depicts a linear relationship between the experimental and predicted values based on the training sets. In general, the selected QSAR models exhibited good agreement ($R^2 \geq 0.81$) between the observed and predicted toxicity for the binary mixtures of MO_X NPs from the training set (blue circle) and those from the test sets (red circle). It can also be seen that the lines of the regression for the N12 and N31 models overlap with the line of perfection, implying that the NN-based models showed better consistency between the experimental and predicted values compared to the SVM-based models. Furthermore, the percental difference averaged between the experimental and predicted values by the NN-based models was 2.17–2.40 and 2.49–2.79 times lower than the percental difference averaged between the experimental and predicted values by the SVM-based models in the internal (Table S7) and combined datasets (Table S8), respectively. Note that the N31 model had the lowest average difference between the experimental and predicted values among the selected QSARs.

In addition, the results for the statistics of the selected models are shown in the insets of Figs. 2 and 3. In the internal dataset (Fig. 2), the S12 model with higher R^2_{adj} and lower RMSE and MAE performed better than the S31 and N12 models for predicting the test data. In addition to this, the NN-based models showed better than the SVM-based models for predicting both the training and test data. Further comparisons revealed that the N31 model with higher R^2_{adj} and lower RMSE and MAE performed better than the N12 model for predicting the test data. In the combined dataset (Fig. 3), the NN-based models with higher R^2_{adj} and lower RMSE and MAE outperformed the SVM-based models for both the training and test data. Of the four models validated, the N31 model with the highest R^2_{adj} and the lowest RMSE and MAE had the best performance capability for predicting the test data. Current research on biological effect prediction also indicates that NN-based models outperform SVM-based models empirically resulting from the training process and overall data prediction (Almansour et al., 2019; Bennett-Lenane et al., 2022), while other studies have shown that the SVM-based modeling approach often shows a better performance than the NN-based approach (Li et al., 2021; Zhao et al., 2006). In theory, both ML algorithms have advantages

Table 2
Toxicity data of binary mixtures of MO_X NPs for the combined dataset [a].

Mixture system of MO_X NPs	Observed log1/EC_{50} (mol/L)	Predicted log1/EC_{50} (mol/L) QSAR models			
		S12	S31	N12	N31
Int (*R*1)					
CuO + ZnO NPs	2.72	2.80	2.89	2.72	2.72
TiO_2 + ZrO_2 NPs	2.10	2.18	2.05	2.10	2.11
ZnO + TiO_2 NPs*	2.17	1.92	2.09	2.21	2.18
ZnO + ZrO_2 NPs	2.30	2.22	2.13	2.30	2.30
CuO + TiO_2 NPs	2.77	2.82	2.94	2.77	2.77
CuO + ZrO_2 NPs	2.29	2.27	2.47	2.27	2.26
Int (*R*2)					
CuO + ZnO NPs*	2.82	2.88	2.92	2.74	2.75
TiO_2 + ZrO_2 NPs*	2.11	2.18	2.05	2.11	2.11
ZnO + TiO_2 NPs	2.20	1.92	2.10	2.19	2.18
ZnO + ZrO_2 NPs*	2.37	2.22	2.13	2.30	2.30
CuO + TiO_2 NPs*	2.74	2.27	2.58	2.05	2.50
CuO + ZrO_2 NPs	2.14	2.22	2.31	2.17	2.19
Ext (*R*3)					
Al_2O_3 + ZnO NPs	4.26	3.93	3.88	4.26	4.26
Al_2O_3 + Fe_2O_3 NPs	2.06	2.14	2.01	2.06	2.07
Al_2O_3 + SiO_2 NPs*	1.71	1.86	1.85	1.88	1.54
Al_2O_3 + TiO_2 NPs	1.70	1.95	1.87	1.71	1.70
ZnO + Fe_2O_3 NPs	3.89	3.81	3.72	3.89	3.89
ZnO + SiO_2 NPs	4.13	3.62	3.57	4.13	4.13
Fe_2O_3 + SiO_2 NPs	2.25	2.17	2.08	2.25	2.25
Fe_2O_3 + TiO_2 NPs*	1.99	1.75	2.10	1.72	2.28
SiO_2 + TiO_2 NPs	1.80	1.88	2.01	1.81	1.80
ZnO + TiO_2 NPs*	4.59	3.76	3.69	4.46	4.01

[a] * indicates the test data.

	χ_{me}							
χ_{me}	S1/N1	$\Sigma\chi_{me/nO}$						
$\Sigma\chi_{me/nO}$	S9/N9	S2/N2	ζP					
ζP	S10/N10	S16/N16	S3/N3	D_H				
D_H	S11/N11	S17/N17	S22/N22	S4/N4	ΔH_{me+}			
ΔH_{me+}	S12/N12	S18/N18	S23/N23	S27/N27	S5/N5	ΔH_{sf}		
ΔH_{sf}	S13/N13	S19/N19	S24/N24	S28/N28	S31/N31	S6/N6	E_C	
E_C	S14/N14	S20/N20	S25/N25	S29/N29	S32/N32	S34/N34	S7/N7	Z^2/r
Z^2/r	S15/N15	S21/N21	S26/N26	S30/N30	S33/N33	S35/N35	S36/N36	S8/N8

Fig. 1. SVM (S1-S36)- and NN (N1-N36)-based QSAR models prepared from the pool of different mixture descriptors. χ_{me} — metal electronegativity, $\Sigma\chi_{me/nO}$ — sum of metal electronegativity for individual metal oxide divided by the number of oxygen atoms present in particular metal oxide, ζP — zeta potential, D_H — hydrodynamic diameters, ΔH_{me+} — enthalpy of formation of a gaseous cation, ΔH_{sf} — metal oxide standard molar enthalpy of formation, E_C — nanoparticle energy of conduction band, and Z^2/r — ionic index of metal cation.

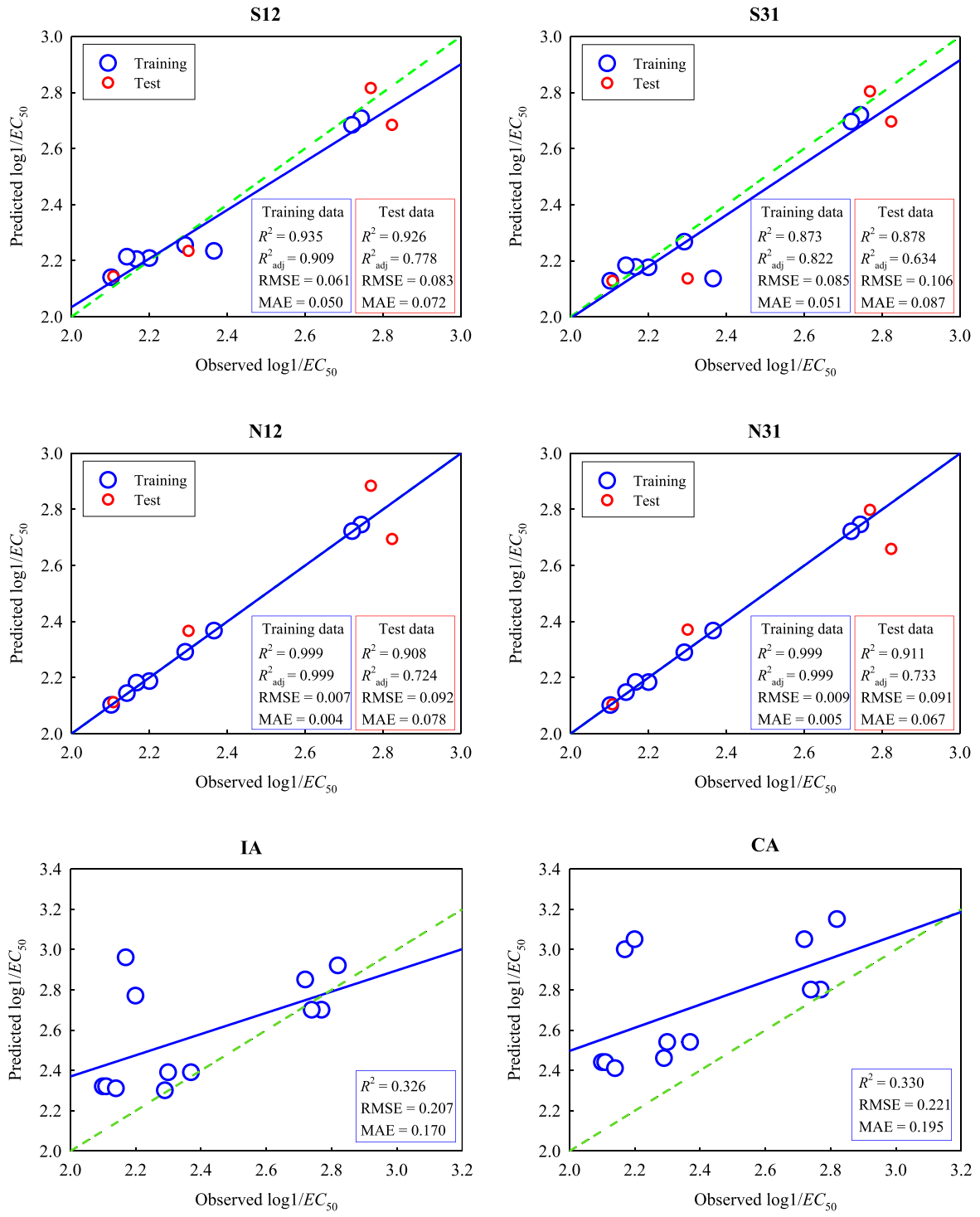

Fig. 2. Performance of the selected SVM- and NN-based QSAR models and the component-based mixture models developed based on the internal dataset.

and disadvantages. This is reflected in that the training time for NN-based technique is higher than the training time for SVM, while the prediction time for NN models is generally lower than for SVM models. Taken together, the performance indicators of the selected QSARs indicate that both the NN and the SVM were practical tools for the prediction of the toxicity of mixtures of ENPs.

To compare the differences between the developed QSAR models and the classical mixture models in predicting the toxicity of mixtures of MO_X NPs, we also constructed the IA and CA prediction models (Figure S1). As shown in Fig. 2, the selected QSAR models gave better predictions of log1/EC_{50} ($R^2 \geq 0.873$) compared to those models based on mixture modeling making use of IA ($R^2 = 0.326$) and CA ($R^2 = 0.330$). This implies that the QSAR models are low-cost approach to risk assessment of multiple ENP mixtures, due to the fact that the QSAR models do not need concentration–response information on each mixture component as with the commonly applied mixture models either using IA or CA. For the CuO + ZrO_2 NPs mixture at ratio 1 and the ZnO + ZrO_2 NPs mixture at ratio 2, the percental difference averaged between the experimental and predicted values by the IA model was lower than the percental difference averaged between the experimental

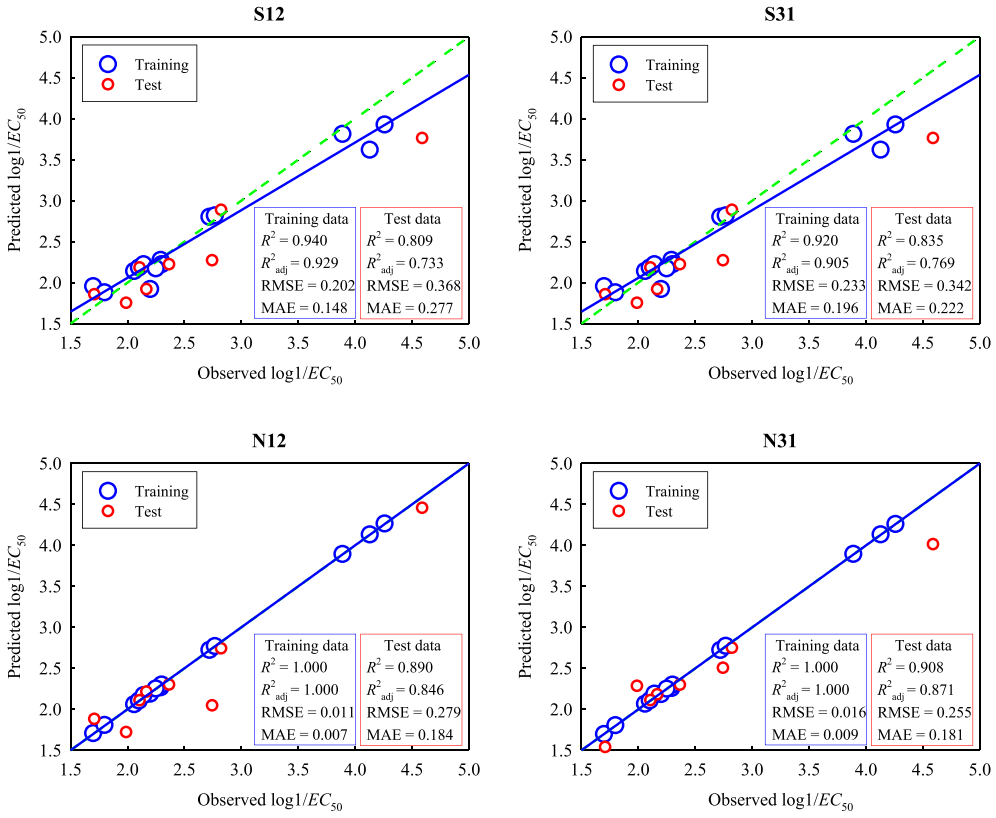

Fig. 3. Performance of the selected SVM- and NN-based QSAR models developed based on the combined dataset.

and predicted values by the SVM-based models (Table S7). This means that for a particular mixture the mixture model has the ability to predict the toxicity of the mixture of MO_X NPs. The mixture model has become a prevailing approach for the quantitative prediction of mixture toxicity with concentration addition being a conservative measure of addition of stress and independent action as assuming induced effects not at the same target and affecting a percentage at the overall response, which strengthens the theorization from the basic principles of mixture

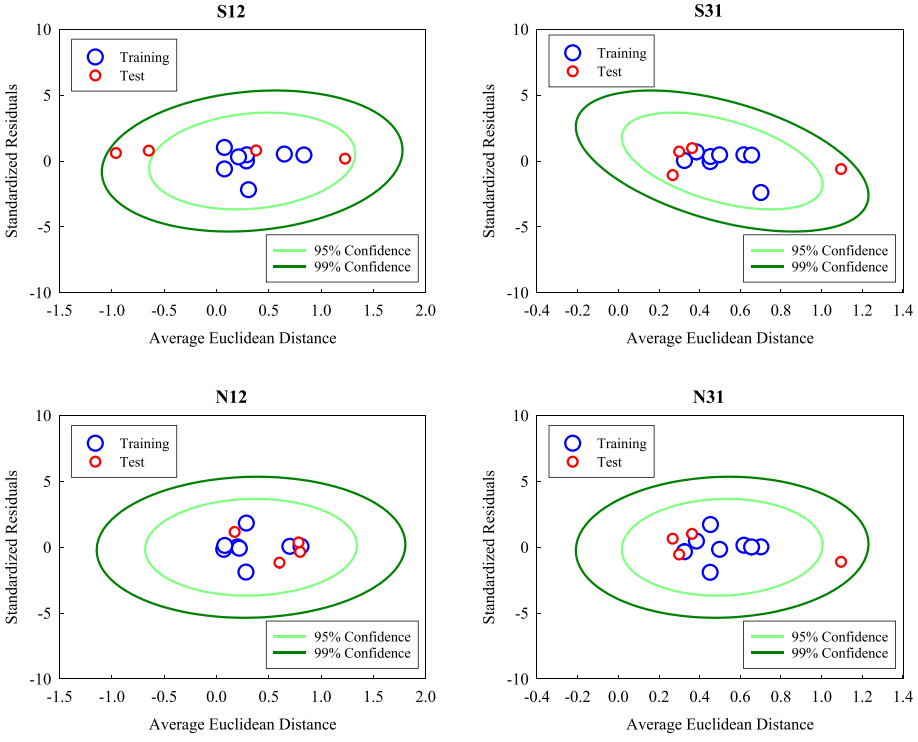

Fig. 4. Applicability domains of the selected SVM- and NN-based QSAR models developed based on the internal dataset.

toxicology. However, the interactions between the joint chemicals are not taken into consideration in the mixture models. Especially, the distinctive physicochemical features of ENPs, which have a high surface area for adsorption, may hinder the mixture models from accurately estimating the toxicological effects of mixtures containing ENPs (Martinez et al., 2022). A previous study indicated that the IA and CA models did not perform well in predicting the toxicity of mixtures comprising TiO_2 NPs and other pollutants to *Daphnia magna* (Trinh et al., 2022). Thus, it is reasonable to assume that the ML-integrated QSAR approach can be considered a highly promising tool for the assessment of the toxicity of a mixture of multiple ENPs.

3.3. Applicability domains of QSAR models

The AD of a QSAR is the physicochemical, structural, or biological space, knowledge or information on which the training set of the model has been developed, and for which it is applicable to make predictions for new compounds (Jaworska et al., 2005). The AD of the SVM-based models (S12 and S31) and NN-based models (N12 and N31) constructed from the internal and combined datasets is shown in Figs. 4 and 5, respectively. The light and dark green elliptical boundaries correspond to the 95 and 99 % confidence intervals, respectively. Reliable predictions can only be generated within these confidence intervals. In the internal dataset (Fig. 4), all the training data fall inside the 95 % confidence area, while two test data for the S12 model and only one test data for the S31 and N31 models falls between 95 and 99 % confidence area. In the combined dataset (Fig. 5), all the training and test data fall inside the 95 % confidence area. Generally, all the studied binary mixtures of MO_X NPs were located within the 99 % confidence area of the selected QSAR models. Thus, the mixture toxicity predictions for each training and test mixtures of MO_X NPs are highly reliable for the selected QSAR models. This suggests that the QSAR models can be used to predict the toxicity of any other binary combinations of MO_X NPs, especially because the predominant first-generation ENPs are within this training set as well as the mechanistically relevant descriptors.

A QSAR model should have a well-defined AD to reflect its reliability in order to be applicable for chemical assessment and management. The dataset with 22 binary combinations has proven to be large and robust to effectively built ML-driven QSAR models for toxicity prediction. This is in line with previous conclusions confirming that ML-assisted QSAR models have good predictive power for relatively small datasets (Gajewicz et al., 2015; Puzyn et al., 2011; Zhong et al., 2022a). These findings do give prospects of application to move the field on mixture toxicity predictions further especially when ENPs mixtures are considered in which chemicals as well as particles influence fate and responses. The characterization of the AD reflects the dependence of a QSAR model on training data (Zhong et al., 2022b). Thus, only nanostructured materials that are similar to the ENPs constituting the training set, can be reliably predicted. While artificial intelligence, ML, and big data analytics provide powerful algorithms and tools for QSAR modeling, high-quality toxicity data remain the driving force for constructing QSAR models for the prediction of the toxicity of nano-mixtures. Therefore, further research needs to expand the amount of high-quality data available on the toxicity of mixtures of ENPs in the training set and enlarge the AD of QSAR models.

3.4. Importance of descriptors and mechanistic knowledge

Table S9 shows the comparative importance of the proposed descriptors for the toxicity prediction of binary mixtures of MO_X NPs. The magnitude of the relative importance of ΔH_{sf} (62 %) and ΔH_{me+} (47 %) is the highest in the internal and combined datasets studied respectively, suggesting that the two descriptors are very important in explaining the QSAR models. As an efficient descriptor, ΔH_{me+} was previously employed to explain the cytotoxicity of MO_X NPs to *E. coli* based on their chemical stability. The chemical stability of MO_X NPs is associated with the release of metal cation from the particles as well as the catalytic properties and redox modifications of the surface (Puzyn et al., 2011). For a given size, ΔH_{sf} might be also used as an indicator of "the ability of releasing metal cation", since it is proportional to the energy of a single metal–oxygen bond in the oxides (Gajewicz et al., 2015). The cellular damage caused by MO_X NPs may be attributed to the release of metal

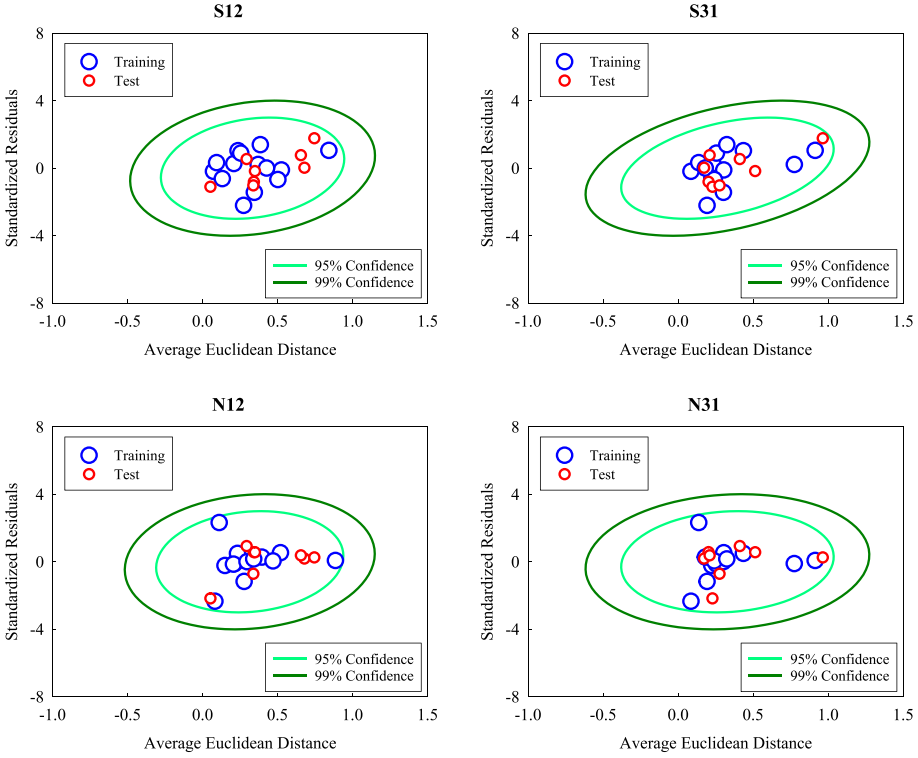

Fig. 5. Applicability domains of the selected SVM- and NN-based QSAR models developed based on the combined dataset.

cations. The metal ions present in suspension can not only chelate with specific ligands of biological macromolecules to affect the toxicity of MO_X NPs to biological cells, but also can instigate the generation of free radicals such as hydroxyl radicals in both cells and mitochondria, causing DNA and mitochondrial DNA breakage (Roy et al., 2019).

In addition, χ_{me} was a significant descriptor in developing the S12 and N12 models, and indicates the energy needed to separate the metal cation from the metal oxides as part of the mechanisms underlying the toxic effects of the metal oxides. MO_X NPs with a higher χ_{me} tend to gain electrons from the bonding pair of the electrons. This indicates an increase in the catalytic capabilities of cationic metal (Roy et al., 2019). Thus, the toxicity of MO_X NPs may be enhanced in accordance with the Haber-Weiss-Fenton cycle (Koppenol, 2001). χ_{me} is also independent of the size range of MO_X NPs (Kar et al., 2014). Following the release of metal cations, redox interactions with the molecules in biological media frequently result in the production of reactive oxygen species (ROS) (Puzyn et al., 2011). Thus, the released cations themselves, ROS-induced oxidative damage, or both may be responsible for the observed cytotoxicity. Our results indicated that these descriptors could indicate possible mechanism for the mixture toxicity of individual MO_X NPs. What is more, the descriptors used in the models are well-defined and can be derived quickly from the chemical composition information (χ_{me}) and chemical stability (ΔH_{me+} and ΔH_{sf}).

The *AICc* values were further applied to evaluate the relationship among the proposed descriptors (χ_{me}, ΔH_{me+}, and ΔH_{sf}). As shown in Table S10, in both the internal dataset and the combined dataset, the *AICc* value of the model developed by applying ΔH_{me+} and ΔH_{sf} was the smallest among all the models combined with the binary descriptors. This indicates that the fitting ability of the model incorporating ΔH_{me+} and ΔH_{sf} was higher than the fitting ability of the other models using the combination of two descriptors. This is generally consistent with the results of the screening and comparative analysis regarding the performance of ML models as described previously. The models developed by applying ΔH_{sf} and ΔH_{me+} to the internal and combined datasets, respectively, had the lowest *AICc* (Table S10). However, the predictive power of the ML models developed by both single descriptors cannot ensure equal predictive power for the internal dataset and the combined dataset (Tables S3 and S4). Furthermore, we found that the *AICc* values of models developed by the combination of three descriptors (χ_{me}, ΔH_{me+}, and ΔH_{sf}) were the highest in the internal dataset, while the *AICc* values of the models developed by the combination of three descriptors in the combined dataset were higher than those of the models developed by the single descriptor (ΔH_{me+}) and the combination of ΔH_{me+} and ΔH_{sf} (Table S10). This implies that applying more descriptors ($n = 3$) to the model in this study could not significantly improve the predictive performance of the model. Furthermore, using fewer descriptors in QSAR analysis not only allows for avoiding overfitting, but also establishes meaningful models with understandable chemical mechanisms (Wang and Chen, 2020). Thereupon, the suggested QSAR models with few utilized nano-descriptors can be regarded as robust and simple to use for predicting the mixture toxicity of ENPs.

4. Conclusions

Our results show that the ML methods present unprecedented opportunities and challenges for the assessment of the mixture toxicity of ENPs. The nano-QSAR models that we developed and validated, outperformed conventional mixture models. The χ_{me}, ΔH_{me+}, and ΔH_{sf} were found to be the key nano-descriptors capable of predicting the mixture toxicity. At the present stage, the synthesis of new NMs and the advanced complexity of materials has a more rapid pace than the science to predict the fate and effects of those complexes and mixtures of ENPs. Knowledge on the mixture impacts of various shaped and chemically diverse ENPs as well as the evaluation of the environmental hazards of combinations of ENPs is a necessity to work on.

CRediT authorship contribution statement

Fan Zhang: Conceptualization, Methodology, Investigation, Data curation, Formal analysis, Writing – original draft, Visualization, Funding acquisition. **Zhuang Wang:** Conceptualization, Formal analysis, Resources, Writing – review & editing, Funding acquisition, Project administration. **Willie J.G.M. Peijnenburg:** Conceptualization, Formal analysis, Writing – review & editing, Supervision, Funding acquisition, Project administration. **Martina G. Vijver:** Conceptualization, Formal analysis, Writing – review & editing, Supervision, Funding acquisition, Project administration.

Declaration of Competing Interest

The authors declare that they have no known competing financial interests or personal relationships that could have appeared to influence the work reported in this paper.

Data availability

Data will be made available on request.

Acknowledgements

The research described in this work was supported by the National Natural Science Foundation of China (grant number 31971522) and by the European Union's Horizon 2020 research and innovation program via the projects "NanoinformaTIX" (grant number 814426). Martina G. Vijver acknowledges the support of the ERC-C grant entitled EcoWizard no. 101002123. Fan Zhang greatly acknowledges the support from the China Scholarship Council (grant number 202008320308).

Appendix A. Supplementary data

Supplementary data to this article can be found online at https://doi.org/10.1016/j.envint.2023.108025.

References

Almansour, N.A., Syed, H.F., Khayat, N.R., Altheeb, R.K., Juri, R.E., Alhiyafi, J., Alrashed, S., Olatunji, S.O., 2019. Neural network and support vector machine for the prediction of chronic kidney disease: A comparative study. Comput. Biol. Med. 109, 101–111. https://doi.org/10.1016/j.compbiomed.2019.04.017.

Altenburger, R., Nendza, M., Schüürmann, G., 2003. Mixture toxicity and its modeling by quantitative structure-activity relationships. Environ. Toxicol. Chem. 22, 1900–1915. https://doi.org/10.1897/01-386.

Avellan, A., Yun, J., Morais, B.P., Clement, E.T., Rodrigues, S.M., Lowry, G.V., 2021. Critical review: Role of inorganic nanoparticle properties on their foliar uptake and *in planta* translocation. Environ. Sci. Technol. 55, 13417–13431. https://doi.org/10.1021/acs.est.1c00178.

Balraadjsing, S., Peijnenburg, W.J.G.M., Vijver, M.G., 2022. Exploring the potential of *in silico* machine learning tools for the prediction of acute *Daphnia magna* nanotoxicity. Chemosphere 307, 135930. https://doi.org/10.1016/j.chemosphere.2022.135930.

Ban, M.J., Lee, D.H., Shin, S.W., Kim, K., Kim, S., Oa, S.-W., Kim, G.-H., Park, Y.-J., Jin, D.R., Lee, M., Kang, J.-H., 2022. Identifying the acute toxicity of contaminated sediments using machine learning models. Environ. Pollut. 312, 120086 https://doi.org/10.1016/j.envpol.2022.120086.

Bennett-Lenane, H., Griffin, B.T., O'Shea, J.P., 2022. Machine learning methods for prediction of food effects on bioavailability: A comparison of support vector machines and artificial neural networks. Eur. J. Pharm. Sci. 168, 106018 https://doi.org/10.1016/j.ejps.2021.106018.

Bliss, C.I., 1939. The toxicity of poisons applied jointly. Ann. Appl. Biol. 26, 585–615. https://doi.org/10.1111/j.1744-7348.1939.tb06990.x.

Demšar, J., Curk, T., Erjavec, A., Gorup, C., Hočevar, T., Milutinovič, M., Možina, M., Polajnar, M., Toplak, M., Starič, A., Štajdohar, M., Umek, L., Žagar, L., Žbontar, J., Žitnik, M., Zupan, B., 2013. Orange: Data mining toolbox in python. J. Mach. Learn. Res. 14, 2349–2353.

Gajewicz, A., 2018. How to judge whether QSAR/read-across predictions can be trusted: A novel approach for establishing a model's applicability domain. Environ. Sci.: Nano 5, 408–421. https://doi.org/10.1039/C7EN00774D.

Gajewicz, A., Schaeublin, N., Rasulev, B., Hussain, S., Leszczynska, D., Puzyn, T., Leszczynski, J., 2015. Towards understanding mechanisms governing cytotoxicity of metal oxides nanoparticles: Hints from nano-QSAR studies. Nanotoxicology 9, 313–325. https://doi.org/10.3109/17435390.2014.930195.

Georgantzopoulou, A., Farkas, J., Ndungu, K., Coutris, C., Carvalho, P.A., Booth, A.M., Macken, A., 2020. Wastewater-aged silver nanoparticles in single and combined exposures with titanium dioxide affect the early development of the marine copepod *Tisbe battagliai*. Environ. Sci. Technol. 54, 12316–12325. https://doi.org/10.1021/acs.est.0c03113.

Haynes, W.M., 2011. CRC Handbook of Chemistry and Physics, 92nd Edition. CRC Press.

Hong, H., Adam, V., Nowack, B., 2021. Form-specific and probabilistic environmental risk assessment of 3 engineered nanomaterials (nano-Ag, nano-TiO_2, and nano-ZnO) in European freshwaters. Environ. Toxicol. Chem. 40, 2629–2639. https://doi.org/10.1002/etc.5146.

Jaworska, J., Nikolova-Jeliazkova, N., Aldenberg, T., 2005. QSAR applicabilty domain estimation by projection of the training set descriptor space: A review. Altern. Lab. Anim. 33, 445–459. https://doi.org/10.1177/026119290503300508.

Jayaramulu, K., Mukherjee, S., Morales, D.M., Dubal, D.P., Nanjundan, A.K., Schneemann, A., Masa, J., Kment, S., Schuhmann, W., Otyepka, M., Zbořil, R., Fischer, R.A., 2022. Graphene-based metal–organic framework hybrids for applications in catalysis, environmental, and energy technologies. Chem. Rev. 122, 17241–17338. https://doi.org/10.1021/acs.chemrev.2c00270.

Ji, Z., Guo, W., Wood, E.L., Liu, J., Sakkiah, S., Xu, X., Patterson, T.A., Hong, H., 2022. Machine learning models for predicting cytotoxicity of nanomaterials. Chem. Res. Toxicol. 35, 125–139. https://doi.org/10.1021/acs.chemrestox.1c00310.

Jia, Y., Hou, X., Wang, Z., Hu, X., 2021. Machine learning boosts the design and discovery of nanomaterials. ACS Sustainable Chem. Eng. 9, 6130–6147. https://doi.org/10.1021/acssuschemeng.1c00483.

Kar, S., Gajewicz, A., Puzyn, T., Roy, K., Leszczynski, J., 2014. Periodic table-based descriptors to encode cytotoxicity profile of metal oxide nanoparticles: A mechanistic QSTR approach. Ecotoxicol. Environ. Saf. 107, 162–169. https://doi.org/10.1016/j.ecoenv.2014.05.026.

Kar, S., Pathakoti, K., Leszczynska, D., Tchounwou, P.B., Leszczynski, J., 2022. *In vitro* and *in silico* study of mixtures cytotoxicity of metal oxide nanoparticles to *Escherichia coli* : A mechanistic approach. Nanotoxicology 16, 566–579. https://doi.org/10.1080/17435390.2022.2123750.

Koppenol, W.H., 2001. The Haber-Weiss cycle-70 years later. REDOX Report: Communications in Free Radical Research 6, 229–234. https://doi.org/10.1179/135100001101536373.

Kubinyi, H., 1993. QSAR: Hansch analysis and related approaches. In: Mann-hold, R., Krogsgaard-Larsen, P., Timmerman, H. (Eds.), Methods and principles in medicinal chemistry, vol 1. VCH, Weinheim. https://doi.org/10.1002/9783527616824.

Li, X., Yang, B., Yang, J., Fan, Y., Qian, X., Li, H., 2021. Magnetic properties and its application in the prediction of potentially toxic elements in aquatic products by machine learning. Sci. Total Environ. 783, 147083 https://doi.org/10.1016/j.scitotenv.2021.147083.

Liu, R., Zhang, H.Y., Ji, Z.X., Rallo, R., Xia, T., Chang, C.H., Nel, A., Cohen, Y., 2013. Development of structure–activity relationship for metal oxide nanoparticles. Nanoscale 5, 5644–5653. https://doi.org/10.1039/c3nr01533e.

Loewe, S., Muischneck, H., 1926. Effect of combinations: Mathematical basis of problem. Arch. Exp. Pathol. Pharmakol. 114, 313–326.

Lopes, S., Pinheiro, C., Soares, A.M.V.M., Loureiro, S., 2016. Joint toxicity prediction of nanoparticles and ionic counterparts: Simulating toxicity under a fate scenario. J. Hazard. Mater. 320, 1–9. https://doi.org/10.1016/j.jhazmat.2016.07.068.

Martín-de-Lucía, I., Gonçalves, S.F., Leganés, F., Fernández-Piñas, F., Rosal, R., Loureiro, S., 2019. Combined toxicity of graphite-diamond nanoparticles and thiabendazole to *Daphnia magna*. Sci. Total Environ. 688, 1145–1154. https://doi.org/10.1016/j.scitotenv.2019.06.316.

Martinez, D.S.T., Ellis, L.-J.-A., Da Silva, G.H., Petry, R., Medeiros, A.M.Z., Davoudi, H. H., Papadiamantis, A.G., Fazzio, A., Afantitis, A., Melagraki, G., Lynch, I., 2022. *Daphnia magna* and mixture toxicity with nanomaterials – Current status and perspectives in data-driven risk prediction. Nano Today 43, 101430. https://doi.org/10.1016/j.nantod.2022.101430.

Mikolajczyk, A., Malankowska, A., Nowaczyk, G., Gajewicz, A., Hirano, S., Jurga, S., Zaleska-Medynska, A., Puzyn, T., 2016. Combined experimental and computational approach to developing efficient photocatalysts based on Au/Pd–TiO_2 nanoparticles. Environ. Sci.: Nano 3, 1425–1435. https://doi.org/10.1039/C6EN00232C.

Na, M., Nam, S.H., Moon, K., Kim, J., 2023. Development of a nano-QSAR model for predicting the toxicity of nano-metal oxide mixtures to *Aliivibrio fischeri*. Environ. Sci.: Nano 10, 325–337. https://doi.org/10.1039/D2EN00672C.

OECD, 2014. Guidance Document on the Validation of (Quantitative) Structure-Activity Relationship [(Q)SAR] Models, OECD Series on Testing and Assessment. OECD. Doi: 10.1787/9789264085442-en.

Olasupo, S.B., Uzairu, A., Shallangwa, G.A., Uba, S., 2020. Chemoinformatic studies on some inhibitors of dopamine transporter and the receptor targeting schizophrenia for developing novel antipsychotic agents. Heliyon 6, e04464. https://doi.org/10.1016/j.heliyon.2020.e04464.

Patton, T., Barrett, J., Brennan, J., Moran, N., 2006. Use of a spectrophotometric bioassay for determination of microbial sensitivity to manuka honey. J. Microbiol. Methods 64, 84–95. https://doi.org/10.1016/j.mimet.2005.04.007.

Puzyn, T., Rasulev, B., Gajewicz, A., Hu, X., Dasari, T.P., Michalkova, A., Hwang, H.-M., Toropov, A., Leszczynska, D., Leszczynski, J., 2011. Using nano-QSAR to predict the cytotoxicity of metal oxide nanoparticles. Nature Nanotech. 6, 175–178. https://doi.org/10.1038/nnano.2011.10.

Roy, K., Kar, S., Das, R.N., 2015. A Primer on QSAR/QSPR Modeling (2015th ed.). Cham: Springer International Publishing AG. Doi:10.1007/978-3-319-17281-1.

Roy, J., Ojha, P.K., Roy, K., 2019. Risk assessment of heterogeneous TiO_2-based engineered nanoparticles (NPs): A QSTR approach using simple periodic table based descriptors. Nanotoxicology 13, 701–716. https://doi.org/10.1080/17435390.2019.1593543.

Simelane, S., Dlamini, L.N., 2019. An investigation of the fate and behaviour of a mixture of WO_3 and TiO_2 nanoparticles in a wastewater treatment plant. J. Environ. Sci. 76, 37–47. https://doi.org/10.1016/j.jes.2018.03.018.

Singh, D., Kumar, A., 2020. Binary mixture of nanoparticles in sewage sludge: Impact on spinach growth. Chemosphere 254, 126794. https://doi.org/10.1016/j.chemosphere.2020.126794.

Trinh, T.X., Seo, M., Yoon, T.H., Kim, J., 2022. Developing random forest based QSAR models for predicting the mixture toxicity of TiO_2 based nano-mixtures to *Daphnia magna*. NanoImpact 25, 100383. https://doi.org/10.1016/j.impact.2022.100383.

Tropsha, A., 2010. Best practices for QSAR model development, validation, and exploitation. Mol. Inform. 29, 476–488. https://doi.org/10.1002/minf.201000061.

Walker, J.D., Enache, M., Dearden, J.C., 2003. Quantitative cationic–activity relationships for predicting toxicity of metals. Environ. Toxicol. Chem. 22, 1916–1935. https://doi.org/10.1897/02-568.

Wang, Y., Chen, X., 2020. A joint optimization QSAR model of fathead minnow acute toxicity based on a radial basis function neural network and its consensus modeling. RSC Adv. 10, 21292–21308. https://doi.org/10.1039/d0ra02701d.

Wang, M., Yu, H.L., Chen, Y., Huang, M.X., 2021. Machine learning assisted screening of non-rare-earth elements for Mg alloys with low stacking fault energy. Comp. Mater. Sci. 196, 110544 https://doi.org/10.1016/j.commatsci.2021.110544.

Wyrzykowska, E., Mikolajczyk, A., Lynch, I., Jeliazkova, N., Kochev, N., Sarimveis, H., Doganis, P., Karatzas, P., Afantitis, A., Melagraki, G., Serra, A., Greco, D., Subbotina, J., Lobaskin, V., Bañares, M.A., Valsami-Jones, E., Jagiello, K., Puzyn, T., 2022. Representing and describing nanomaterials in predictive nanoinformatics. Nat. Nanotechnol. 17, 924–932. https://doi.org/10.1038/s41565-022-01173-6.

Yang, L., Chen, P., He, K., Wang, R., Chen, G., Shan, G., Zhu, L., 2022. Predicting bioconcentration factor and estrogen receptor bioactivity of bisphenol a and its analogues in adult zebrafish by directed message passing neural networks. Environ. Int. 169, 107536 https://doi.org/10.1016/j.envint.2022.107536.

Zhang, H., Ji, Z., Xia, T., Meng, H., Low-Kam, C., Liu, R., Pokhrel, S., Lin, S., Wang, X., Liao, Y.-P., Wang, M., Li, L., Rallo, R., Damoiseaux, R., Telesca, D., Mädler, L., Cohen, Y., Zink, J.I., Nel, A.E., 2012. Use of metal oxide nanoparticle band gap to develop a predictive paradigm for oxidative stress and acute pulmonary inflammation. ACS Nano 6, 4349–4368. https://doi.org/10.1021/nn3010087.

Zhang, F., Wang, Z., Vijver, M.G., Peijnenburg, W.J.G.M., 2021. Prediction of the joint toxicity of multiple engineered nanoparticles: The integration of classic mixture models and *in silico* methods. Chem. Res. Toxicol. 34, 176–178. https://doi.org/10.1021/acs.chemrestox.0c00300.

Zhang, F., Wang, Z., Peijnenburg, W.J.G.M., Vijver, M.G., 2022a. Review and prospects on the ecotoxicity of mixtures of nanoparticles and hybrid nanomaterials. Environ. Sci. Technol. 56, 15238–15250. https://doi.org/10.1021/acs.est.2c03333.

Zhang, F., Wang, Z., Vijver, M.G., Peijnenburg, W.J.G.M., 2022b. Theoretical investigation on the interactions of microplastics with a SARS-CoV-2 RNA fragment and their potential impacts on viral transport and exposure. Sci. Total Environ. 842, 156812 https://doi.org/10.1016/j.scitotenv.2022.156812.

Zhao, C.Y., Zhang, H.X., Zhang, X.Y., Liu, M.C., Hu, Z.D., Fan, B.T., 2006. Application of support vector machine (SVM) for prediction toxic activity of different data sets. Toxicology 217, 105–119. https://doi.org/10.1016/j.tox.2005.08.019.

Zhong, S., Zhang, Y., Zhang, H., 2022a. Machine learning-assisted QSAR models on contaminant reactivity toward four oxidants: Combining small data sets and knowledge transfer. Environ. Sci. Technol. 56, 681–692. https://doi.org/10.1021/acs.est.1c04883.

Zhong, S., Lambeth, D.R., Igou, T.K., Chen, Y., 2022b. Enlarging applicability domain of quantitative structure–activity relationship models through uncertainty-based active learning. ACS EST Eng. 2, 1211–1220. https://doi.org/10.1021/acsestengg.1c00434.